

A Novel Dimeric Ni-Substituted β -Keggin Silicotungstate: Structure and Magnetic Properties of $K_{12}[\{\beta\text{-SiNi}_2\text{W}_{10}\text{O}_{36}(\text{OH})_2(\text{H}_2\text{O})\}_2]\cdot 20\text{H}_2\text{O}$

Ulrich Kortz,^{*,†,‡} Yves P. Jeannin,[§] André Tézé,[†] Gilbert Hervé,[†] and Samih Isber^{||}

Institut de Réactivité, Électrochimie et Microporosités, UMR C0173, Université de Versailles, 45 Avenue des États Unis, 78035 Versailles Cedex, France, Laboratoire de Chimie des Métaux de Transition, ESA-CNRS 7071, Université Pierre et Marie Curie, 4, Place Jussieu, 75252 Paris Cedex 05, France, and Department of Physics, American University of Beirut, Bliss Street, P.O. Box 11-0236, Beirut, Lebanon

Received January 6, 1999

The novel dimeric polyoxometalate $[\{\beta\text{-SiNi}_2\text{W}_{10}\text{O}_{36}(\text{OH})_2(\text{H}_2\text{O})\}_2]^{12-}$ (**1**) has been synthesized and characterized by IR spectroscopy, polarography, elemental analysis, thermogravimetric analysis, and magnetic measurements. An X-ray single-crystal analysis was carried out on $K_{12}[\{\beta\text{-SiNi}_2\text{W}_{10}\text{O}_{36}(\text{OH})_2(\text{H}_2\text{O})\}_2]\cdot 20\text{H}_2\text{O}$, which crystallizes in the monoclinic system, space group $P2_1/n$, with $a = 13.701(4)$ Å, $b = 24.448(11)$ Å, $c = 13.995(5)$ Å, $\beta = 99.62(3)^\circ$, and $Z = 4$. The anion consists of two $[\beta\text{-SiNi}_2\text{W}_{10}\text{O}_{36}(\text{OH})_2(\text{H}_2\text{O})]$ Keggin moieties linked via two OH bridging groups, leading to a planar $\text{Ni}_2(\text{OH})_2$ unit. The two half-units are related by an inversion center and each contain one Ni atom in the rotated triad. The formation of the new anion involves insertion, isomerization, and dimerization. Magnetic measurements show that the central Ni_4 unit exhibits ferromagnetic ($J' = 4.14 \text{ cm}^{-1}$) as well as weak antiferromagnetic ($J = -0.65 \text{ cm}^{-1}$) Ni–Ni exchange interactions.

Introduction

Polyoxometalates exhibit an enormous variety of structures, which leads to interesting and often unexpected properties in fields such as magnetochemistry, catalysis and medicine.^{1–4} The mechanism of the formation of polyoxometalates, however, is still not well understood and is often described as self-assembly. Nevertheless, the reaction of stable lacunary polyoxometalates with transition metal ions usually leads to a monomeric or dimeric product with the heteropolyanion framework unchanged.⁵ Lacunary polyoxoanions can therefore be regarded as bulky polydentate ligands and, depending upon the coordination requirement and the size of a given transition metal ion, the geometry of the reaction product can often be predicted.

However, if the lacunary polyoxoanion is metastable, dissolution of the species initiates isomerization. The isomerization behavior of silicotungstates in aqueous solution has been studied by Tézé et al. and is quite well understood.⁶ Reaction of lacunary, metastable silicotungstates with transition metal ions has led to mono-, di-, and trisubstituted products.⁷ The challenge is to understand the impact of a given transition metal ion on the isomerization processes of silicotungstates.⁸

Transition metal-substituted polyoxometalates can be of interest for their magnetic properties if a number of paramagnetic metal ions (e.g. Ni^{2+} , Co^{2+}) are ferromagnetically spin-coupled leading to materials intermediate between those of isolated ions and bulk magnetic materials.^{9,10} Usually, the paramagnetic motifs are well-isolated from each other by the heteropolyanion frameworks. The challenge has been to synthesize polyoxoanions that contain a number of transition metal ions and some examples of di- and trisubstituted silicotungstates have been reported.^{7b–e} Because there were no reports on di nickel substituted silicotungstates, we decided to investigate this

* Corresponding author. E-mail: ulrich.kortz@aub.edu.lb.

† Université de Versailles.

§ Université Pierre et Marie Curie.

|| American University of Beirut.

‡ Present address: Department of Chemistry, American University of Beirut, Bliss Street, P.O. Box 11–0236, Beirut, Lebanon.

(1) *Chem. Rev., Polyoxometalates*, C. Hill, Ed. 1998.

(2) *Polyoxometalates: from Platonic Solids to Anti-Retroviral Activity*, Pope, M. T., Müller, A., Eds.; Kluwer: Dordrecht, The Netherlands, 1994.

(3) Pope, M. T.; Müller, A. *Angew. Chem., Int. Ed. Engl.* **1991**, *30*, 34–48.

(4) Pope, M. T. *Heteropoly and Isopoly Oxometalates*, Springer-Verlag, Berlin, 1983.

(5) (a) Weakley, T. J. R.; Evans, H. T. jun.; Showell, J. S.; Tourné, G. F.; Tourné, C. M. *J. Chem. Soc., Chem. Commun.* **1973**, 139. (b) Finke, R. G.; Weakley, T. J. R. *Inorg. Chem.* **1990**, *29*, 1235. (c) Knoth, W. H.; Domaille, P. J.; Farlee, R. D. *Organometallics* **1985**, *4*, 62. (d) Knoth, W. H.; Domaille, P. J.; Harlow, R. L. *Inorg. Chem.* **1986**, *25*, 1577. (e) Finke, R. G.; Droegge, M. W.; Domaille, P. J. *Inorg. Chem.* **1987**, *26*, 3886. (f) Gómez-García, C. J.; Coronado, E.; Borrás-Almenar, J. J. *Inorg. Chem.* **1992**, *31*, 1667. (g) Casañ-Pastor, N.; Bas, J.; Coronado, E.; Pourroy, G.; Baker, L. C. W. *J. Am. Chem. Soc.* **1992**, *114*, 10380. (h) Gómez-García, C. J.; Borrás-Almenar, J. J.; Coronado, E.; Ouahab, L. *Inorg. Chem.* **1994**, *33*, 4016.

(6) Tézé, A.; Hervé, G. *Inorganic Syntheses*, John Wiley & Sons: New York, 1990; Vol. 27, p 85.

(7) (a) Tézé, A.; Hervé, G. *J. Inorg. Nucl. Chem.* **1977**, *39*, 2151. (b)

Wassermann, K.; Lunk, H.-J.; Palm, R.; Fuchs, J.; Steinfeldt, N.; Stösser, R.; Pope, M. T. *Inorg. Chem.* **1996**, *35*, 3273. (c) Zhang, X.-Y.; O'Connor, C. J.; Jameson, G. B.; Pope, M. T. *Inorg. Chem.* **1996**, *35*, 30. (d) Xin, F.; Pope, M. T. *Inorg. Chem.* **1996**, *35*, 5693. (e) Liu, J.; Ortéga, F.; Sethuraman, P.; Katsoulis, D. E.; Costello, C. E.; Pope, M. T. *J. Chem. Soc., Dalton Trans.* **1992**, 1901.

(8) Canny, J.; Thouvenot, R.; Tézé, A.; Hervé, G.; Leparulo-Loftus, M.; Pope, M. T. *Inorg. Chem.* **1991**, *30*, 976.

(9) Gatteschi, D. *Adv. Mater.* **1994**, *6*, 635.

(10) *Magnetic Molecular Materials*, Gatteschi, D., Kahn, O., Müller, J. S., Palacio, F., Eds.; Kluwer: Dordrecht, The Netherlands, 1991.

(11) (a) Clemente-Juan, J. M.; Coronado, E.; Galán-Mascarós, J. R.; Gómez-García, C. J. *Inorg. Chem.* **1999**, *38*, 55. (b) Coronado, E.; Gómez-García, C. J. *Comments Inorg. Chem.* **1995**, *17*, 255.

(12) Gómez-García, C. J.; Coronado, E.; Ouahab, L. *Angew. Chem., Int. Ed. Engl.* **1992**, *31*, 649.

(13) Kortz, U.; Tézé, A.; Hervé, G. *Inorg. Chem.* **1999**, *38*, 2038.

system, knowing that the Ni–Ni exchange interactions in Ni substituted polyoxometalates are usually ferromagnetic.^{11–13}

Experimental Section

Synthesis. A 2.38 g sample of $K_8[\gamma\text{-SiW}_{10}\text{O}_{36}]$ (synthesized according to Tézé et al.¹⁴ identity and purity of the lacunary precursor ion were verified by polarography and IR spectroscopy, and they were in complete agreement with the characteristics given by Canny et al.¹⁵) was added with stirring to a solution of 0.48 g $\text{NiSO}_4 \cdot 6\text{H}_2\text{O}$ in 20 mL of a 0.5 M potassium acetate buffer (pH 4.8). This solution was heated to 50 °C for 45 min and then cooled to room temperature. Addition of solid KCl led to a light green precipitate which was collected in a sintered-glass frit and air-dried. Yield was 1.25 g (50%). The crude material was dissolved in H_2O , and, upon standing in a refrigerator for a few weeks, green single-crystalline needles suitable for X-ray crystallography were obtained. Anal. Calcd for $K_{12}[\{\beta\text{-SiNi}_2\text{W}_{10}\text{O}_{36}(\text{OH})_2(\text{H}_2\text{O})\}_2] \cdot 30\text{H}_2\text{O}$: K, 7.53; W, 58.99; Ni, 3.77; Si, 0.90. Found: K, 7.39; W, 58.81; Ni, 3.75; Si, 1.09. Thermogravimetric analysis is in full accordance with the elemental analysis. Elemental analysis was performed by the Service Central d'Analyse of CNRS at 69390 Vernaison, France. IR (KBr pellet; cm^{-1}): 987 (m), 962 (sh), 949 (s), 891 (vs), 862 (sh), 794 (vs), 742 (s), 706 (sh), 542 (w), 520 (w). For comparison, the IR spectra of $K_4[\beta\text{-SiW}_{12}\text{O}_{40}] \cdot 9\text{H}_2\text{O}$ and $K_4[\alpha\text{-SiW}_{12}\text{O}_{40}] \cdot 17\text{H}_2\text{O}$ are (KBr pellet; cm^{-1}): 1018, 984, 917, 865, 791, 550 (sh), 530, 510 (sh), 427 and 1020, 999, 980, 940 (sh), 925, 894, 878, 780, 550 (sh), 530, 474, 413, respectively.

X-ray Crystallography. A light green needle with dimensions $0.40 \times 0.35 \times 0.25 \text{ mm}^3$ was stuck on a glass fiber and mounted on an Enraf-Nonius CAD4 automatic diffractometer. Preliminary examination and data collection were performed at room temperature with Mo $K\alpha$ radiation ($\lambda = 0.71069 \text{ \AA}$). Cell constants and an orientation matrix for data collection were obtained from the least-squares refinement of the setting angles of 25 reflections. During data collection, three standard reflections were measured every hour and showed no significant decay. Lorentz polarization and absorption correction (DIFABS) were applied to the intensity data.¹⁶ On the basis of systematic absences and statistics of intensity distribution, the space group was found to be $P2_1/n$. The structure was determined, and heavy atoms were found by direct methods using SHELXS 86.¹⁷ All the remaining atoms were found after successive full-matrix least-squares refinements and Fourier syntheses. The final refinement was carried out by inverting the full-matrix and introducing anisotropic thermal parameters for W, Ni, K and Si, taking into account secondary extinction and anomalous dispersion. Hydrogen atoms were not included. Only the 5390 reflections with $I > 3\sigma(I)$ were used in refinement, which converged at $R = 0.046$ and $R_w = 0.054$. In the final difference map, the deepest hole was -2.5 e \AA^{-3} and the highest peak 3.6 e \AA^{-3} . All computations were performed using the CRYSTALS package.¹⁸ Crystallographic data are summarized in Table 1, and positional parameters are shown in Table 2. Bond lengths of the dimeric polyoxometalate, **1**, are given in Table 3.

Spectral and Magnetic Measurements. The IR spectrum was recorded on a Nicolet 550 FTIR spectrophotometer in a KBr pellet. Thermogravimetric analysis was performed with a Perkin-Elmer TGA7 instrument. The polarogram was obtained in a sodium acetate buffer solution (1 M, pH 4.8). The magnetic measurements were carried out with a SQUID magnetometer in the temperature range 2–290 K up to 50 kG.

Results and Discussion

Structure of $K_{12}[\{\beta\text{-SiNi}_2\text{W}_{10}\text{O}_{36}(\text{OH})_2(\text{H}_2\text{O})\}_2] \cdot 20\text{H}_2\text{O}$. The novel polyoxoanion **1** can be described as a dimer of Keggin

Table 1. Crystal Data and Structure Refinement for $K_{12}[\{\beta\text{-SiNi}_2\text{W}_{10}\text{O}_{36}(\text{OH})_2(\text{H}_2\text{O})\}_2] \cdot 20\text{H}_2\text{O}$

chem formula	$K_6\text{SiW}_{10}\text{Ni}_2\text{O}_{49}\text{H}_{24}$
fw	3026.74
space group (No.)	$P2_1/n$ (14)
unit cell dimensions	$a = 13.701(4) \text{ \AA}$ $b = 24.448(11) \text{ \AA}$ $c = 13.995(5) \text{ \AA}$ $\beta = 99.62(3)^\circ$
volume	$4622(3) \text{ \AA}^3$
Z	4
temperature	22 °C
wavelength	0.71069 Å
density (calculated)	4.35 g/cm^3
absorption coefficient	268 cm^{-1}
$R(F_o)^a$	0.046
$R_w(F_o)^b$	0.054

$$^a R = \sum |F_o| - |F_c| / \sum |F_o|. \quad ^b R_w = (\sum w(|F_o| - |F_c|)^2 / \sum w|F_o|^2)^{1/2}.$$

ions (see Figures 1 and 2).¹⁹ Two lacunary $[\beta\text{-SiW}_{10}\text{O}_{37}]^{10-}$ units, which accommodate two Ni^{2+} ions each, are linked through two triply bridging OH groups. Since the half-units are related by an inversion center, there are only two structurally nonequivalent types of Ni in **1** (Ni1 and Ni2). Ni1 is located in the rotated triad Ni1–W3–W9 of each half unit; Ni2 is in an adjacent triad Ni2–W5–W10 and shares the O1 oxygen atom with Ni1. Each Ni is in a distorted octahedral coordination environment, and dimerization of the two-half units is accomplished through sharing of two O1 atoms, the same oxygens that also bridge the two Ni ions in each half-unit. These two triply bridging oxygen atoms (O1 and O1') are symmetry-related by the inversion center of **1** and are bound to both Ni's of one-half-unit and, at the same time, to one Ni of the other half-unit (Distances are Ni1–O1 = 2.07(2), Ni1'–O1 = 2.07(2), and Ni2–O1 = 2.04(2) Å; see Figure 3). The geometry of the central Ni_4 core of **1** is unique because Ni1, O1, Ni1' and O1' form a perfectly planar parallelogram (Ni1–O1–Ni1' $93.8(7)^\circ$, O1–Ni1–O1' $86.2(7)^\circ$), and the two bonds O1–Ni2 and O1'–Ni2' are on opposite sides of the planar unit, with which they form an angle of 141.6° . Thereby, all four Ni atoms are linked through only two μ_3 -oxygens.

The two half-units of **1** deserve special attention because they contain $[\beta\text{-SiW}_{10}\text{O}_{37}]^{10-}$ ions. These ions accommodate two Ni atoms each, leading to complete β -Keggin ions (see Figure 2). According to the IUPAC numbering rules, one-half unit of **1** should be written as $[\beta(4,10)\text{-SiNi}_2\text{W}_{10}\text{O}_{36}(\text{OH})_2(\text{H}_2\text{O})]$, with the numbers 4 and 10 indicating the positions of the Ni atoms.^{1,20}

When reacting $[\gamma\text{-SiW}_{10}\text{O}_{36}]^{8-}$ with Ni^{2+} ions in aqueous solution, we originally expected a dinickel-substituted γ -Keggin product analogous to the dichromium, dimanganese and divanadium γ -Keggin ions reported or perhaps a dimeric anion linked through two Ni ions, analogous to a recently published organotin structure.^{7b–d,8} However, we have not been able to isolate any nickel-substituted γ -silicodectungstate. Hervé et al. reported the synthesis of $[\gamma\text{-SiW}_{10}\text{V}_2\text{O}_{40}]^{6-}$ and the isomerization of the polyanion in aqueous solution.⁸ Depending on the pH, three monomeric β -isomers could be identified, $[\beta(3,12)\text{-SiW}_{10}\text{V}_2\text{O}_{40}]^{6-}$, $[\beta(8,12)\text{-SiW}_{10}\text{V}_2\text{O}_{40}]^{6-}$ and $[\beta(3,8)\text{-SiW}_{10}\text{V}_2\text{O}_{40}]^{6-}$.

Since the reactants for the synthesis of **1** are $[\gamma\text{-SiW}_{10}\text{O}_{36}]^{8-}$ and Ni^{2+} , isomerization of the silicotungstate must occur during the reaction, and it is most likely initiated by the presence of Ni^{2+} ions. This is supported by the fact that the final product **1** is a dimer that is linked through the Ni atoms. Therefore, the

- (14) Tézé, A.; Hervé, G. *Inorganic Syntheses*, John Wiley & Sons: New York, **1990**; Vol. 27, p 88.
 (15) Canny, J.; Tézé, A.; Thouvenot, R.; Hervé, G. *Inorg. Chem.* **1986**, 25, 2114.
 (16) Walker, N.; Stuart, D. *Acta Crystallogr.* **1983**, A39, 158.
 (17) Sheldrick, G. M. *SHELXS 86: Program for Crystal Structure Determination*; University of Göttingen: Göttingen, 1986.
 (18) Watkin, D. J.; Carruthers, J. R.; Betteridge, P. W. *CRYSTALS: An Advanced Crystallographic Computer Program*; Chemical Crystallography Laboratory: Oxford, England, 1989.

(19) Keggin, J. F. *Nature* **1933**, 131, 908.

(20) Jeannin, Y.; Fournier, M. *Pure Appl. Chem.* **1987**, 59, 1529.

Table 2. Fractional Atomic Coordinates and Equivalent Isotropic Displacement Parameters for $K_{12}[\{\beta\text{-SiNi}_2\text{W}_{10}\text{O}_{36}(\text{OH})_2(\text{H}_2\text{O})\}_2] \cdot 20\text{H}_2\text{O}$

atom	<i>x/a</i>	<i>y/b</i>	<i>z/c</i>	<i>U</i> (eq) ^a
W(1)	0.86192(8)	0.19378(4)	0.61688(8)	0.0147
W(2)	0.86174(8)	0.06442(4)	0.54114(7)	0.0138
W(3)	0.63219(8)	0.14458(4)	0.46861(7)	0.0139
W(4)	0.70705(8)	0.22851(4)	0.80376(7)	0.0140
W(5)	0.81189(8)	-0.01608(4)	0.85111(7)	0.0139
W(6)	0.96674(8)	0.09470(5)	0.76852(8)	0.0145
W(7)	0.56703(8)	0.13580(5)	0.88801(7)	0.0147
W(8)	0.81192(8)	0.12723(4)	0.95036(7)	0.0144
W(9)	0.49035(8)	0.17499(4)	0.63330(7)	0.0143
W(10)	0.56112(8)	-0.00589(4)	0.79207(7)	0.0135
Ni(1)	0.5077(2)	0.0529(1)	0.5559(2)	0.0151
Ni(2)	0.7073(2)	-0.0359(1)	0.6368(2)	0.0150
Si(1)	0.7065(5)	0.0959(3)	0.7073(5)	0.0129
K(1)	0.6305(6)	0.4254(3)	0.0447(6)	0.0371
K(2)	0.5871(7)	0.1529(4)	0.1598(5)	0.0458
K(3)	0.7130(6)	0.8808(4)	0.1777(6)	0.0475
K(4)	0.0159(6)	0.7639(3)	0.1252(5)	0.0329
K(5)	0.8864(7)	0.0170(3)	0.1151(6)	0.0392
K(6)	0.0449(8)	0.1588(5)	0.1939(7)	0.0553
atom	<i>x/a</i>	<i>y/b</i>	<i>z/c</i>	<i>U</i> (iso)
O(1)	0.397(1)	0.0077(7)	0.474(1)	0.013(3)
O(2)	0.599(1)	-0.0658(7)	0.706(1)	0.016(4)
O(3)	0.728(1)	-0.1062(8)	0.566(1)	0.021(4)
O(4)	0.808(1)	-0.0611(7)	0.751(1)	0.019(4)
O(5)	0.618(1)	0.1123(7)	0.623(1)	0.015(4)
O(6)	0.912(1)	0.0292(7)	0.803(1)	0.013(4)
O(7)	0.681(1)	0.1273(8)	0.986(1)	0.027(4)
O(8)	0.539(1)	0.0920(8)	0.436(1)	0.027(5)
O(9)	0.419(1)	0.1172(8)	0.579(1)	0.023(4)
O(10)	0.541(1)	0.1933(7)	0.517(1)	0.015(4)
O(11)	0.808(1)	0.2200(8)	0.730(1)	0.021(4)
O(12)	0.698(1)	0.0305(8)	0.737(1)	0.023(4)
O(13)	0.811(1)	0.1077(7)	0.673(1)	0.018(4)
O(14)	0.606(1)	0.2106(7)	0.884(1)	0.016(4)
O(15)	0.701(1)	0.1336(6)	0.802(1)	0.007(3)
O(16)	0.800(1)	0.0543(7)	0.928(1)	0.017(4)
O(17)	0.683(1)	-0.0337(8)	0.878(1)	0.022(4)
O(18)	0.889(1)	-0.0488(7)	0.943(1)	0.017(4)
O(19)	0.911(1)	0.1280(7)	0.868(1)	0.019(4)
O(20)	0.401(1)	0.2261(8)	0.632(1)	0.027(4)
O(21)	0.794(1)	0.2037(7)	0.917(1)	0.019(4)
O(22)	0.565(1)	0.0594(8)	0.866(1)	0.025(4)
O(23)	0.906(1)	0.1436(8)	0.535(1)	0.026(4)
O(24)	0.973(1)	0.0645(9)	0.646(1)	0.029(5)
O(25)	0.811(1)	0.0038(8)	0.577(1)	0.024(4)
O(26)	0.608(1)	0.2185(7)	0.698(1)	0.016(4)
O(27)	0.911(1)	0.2539(8)	0.584(1)	0.019(4)
O(28)	0.919(1)	0.0420(8)	0.446(1)	0.024(4)
O(29)	0.635(1)	0.1768(7)	0.360(1)	0.018(4)
O(30)	0.710(1)	0.2961(8)	0.823(1)	0.024(4)
O(31)	0.971(1)	0.1661(8)	0.714(1)	0.020(4)
O(32)	0.490(1)	0.0218(7)	0.688(1)	0.018(4)
O(33)	0.741(1)	0.0950(8)	0.474(1)	0.022(4)
O(34)	0.882(1)	0.1307(8)	1.064(1)	0.025(4)
O(35)	0.496(1)	0.1469(8)	0.762(1)	0.020(4)
O(36)	1.090(1)	0.0856(9)	0.816(1)	0.029(5)
O(37)	0.476(1)	-0.0429(8)	0.839(1)	0.020(4)
O(38)	0.479(1)	0.1409(8)	0.960(1)	0.023(4)
O(39)	0.734(1)	0.1916(9)	0.550(1)	0.029(5)
O(101)	0.663(2)	0.336(1)	0.161(2)	0.056(7)
O(102)	-0.009(2)	0.0640(9)	0.278(2)	0.034(5)
O(103)	0.419(2)	0.174(1)	0.247(2)	0.045(6)
O(104)	0.687(2)	0.985(1)	0.083(2)	0.056(7)
O(105)	0.120(3)	0.193(1)	0.029(3)	0.08(1)
O(106)	0.783(2)	0.471(1)	0.181(2)	0.061(8)
O(107)	0.709(3)	0.766(2)	0.139(3)	0.11(1)
O(108)	0.742(3)	0.591(2)	0.250(3)	0.09(1)
O(109)	0.706(2)	0.234(1)	0.098(2)	0.066(8)
O(110)	0.709(2)	-0.138(1)	0.965(2)	0.059(7)

^a *U*(eq) is defined as one-third of the trace of the orthogonalized U_{ij} tensor.

Table 3. Bond Distances (Å) of $[\{\beta\text{-SiNi}_2\text{W}_{10}\text{O}_{36}(\text{OH})_2(\text{H}_2\text{O})\}_2]^{12-}$

W(1)–O(11)	1.96(2)	W(7)–O(15)	2.36(1)
W(1)–O(13)	2.39(2)	W(7)–O(22)	1.89(2)
W(1)–O(23)	1.85(2)	W(7)–O(35)	1.88(2)
W(1)–O(27)	1.71(2)	W(7)–O(38)	1.71(2)
W(1)–O(31)	1.96(2)	W(8)–O(7)	1.94(2)
W(1)–O(39)	1.85(2)	W(8)–O(15)	2.36(1)
W(2)–O(13)	2.33(2)	W(8)–O(16)	1.81(2)
W(2)–O(23)	2.03(2)	W(8)–O(19)	1.92(2)
W(2)–O(24)	1.93(2)	W(8)–O(21)	1.93(2)
W(2)–O(25)	1.75(2)	W(8)–O(34)	1.71(2)
W(2)–O(28)	1.74(2)	W(9)–O(10)	1.92(2)
W(2)–O(33)	1.92(2)	W(9)–O(5)	2.34(2)
W(3)–O(8)	1.82(2)	W(9)–O(9)	1.81(2)
W(3)–O(10)	1.94(2)	W(9)–O(20)	1.75(2)
W(3)–O(5)	2.34(2)	W(9)–O(26)	2.02(2)
W(3)–O(29)	1.72(2)	W(9)–O(35)	1.92(2)
W(3)–O(33)	1.91(2)	W(10)–O(2)	2.02(2)
W(3)–O(39)	2.00(2)	W(10)–O(12)	2.32(2)
W(4)–O(11)	1.87(2)	W(10)–O(17)	2.00(2)
W(4)–O(14)	1.98(2)	W(10)–O(22)	1.90(2)
W(4)–O(15)	2.32(2)	W(10)–O(32)	1.75(2)
W(4)–O(21)	1.91(2)	W(10)–O(37)	1.69(2)
W(4)–O(26)	1.85(2)	Ni(1)–O(1)	2.07(2)
W(4)–O(30)	1.67(2)	Ni(1)–O(1)	2.06(2)
W(5)–O(4)	1.77(2)	Ni(1)–O(8)	2.04(2)
W(5)–O(6)	1.97(2)	Ni(1)–O(5)	2.19(2)
W(5)–O(12)	2.34(2)	Ni(1)–O(9)	2.04(2)
W(5)–O(16)	2.05(2)	Ni(1)–O(32)	2.05(2)
W(5)–O(17)	1.92(2)	Ni(2)–O(1)	2.04(2)
W(5)–O(18)	1.71(2)	Ni(2)–O(4)	2.03(2)
W(6)–O(6)	1.86(2)	Ni(2)–O(2)	2.03(2)
W(6)–O(13)	2.34(2)	Ni(2)–O(3)	2.03(2)
W(6)–O(19)	1.88(2)	Ni(2)–O(12)	2.16(2)
W(6)–O(24)	1.89(2)	Ni(2)–O(25)	2.01(2)
W(6)–O(31)	1.91(2)	Si(1)–O(5)	1.60(2)
W(6)–O(36)	1.72(2)	Si(1)–O(12)	1.66(2)
W(7)–O(7)	1.91(2)	Si(1)–O(13)	1.61(2)
W(7)–O(14)	1.91(2)	Si(1)–O(15)	1.63(2)

mechanism for the reaction of Ni^{2+} with $[\gamma\text{-SiW}_{10}\text{O}_{36}]^{8-}$ most likely involves insertion of one or two Ni ions in the lacunary sites of the polyanion, leading to a mono- or dinickel substituted γ -Keggin ion. This ion isomerizes by rotation of one Ni-containing triad by 60° , and dimerization then leads to the final product **1**.

It might be helpful to remember that $[\gamma\text{-SiW}_{10}\text{O}_{36}]^{8-}$ is synthesized by careful hydrolysis of $[\beta_2\text{-SiW}_{11}\text{O}_{39}]^{8-}$, in which the lacunary site is adjacent to the rotated triad (see Figure 4).⁶ This means that the synthesis of the γ -silicododecatungstate ion is accompanied by isomerization. Starting with $[\beta_2\text{-SiW}_{11}\text{O}_{39}]^{8-}$, one can imagine that first a WO_2^{2+} fragment is lost from the rotated triad, and the fragment must originate from the WO_6 octahedron next to the lacunary site. The intermediate anion thereby formed is $[\beta\text{-SiW}_{10}\text{O}_{37}]^{10-}$. It can be pointed out that this species has a high negative charge and that one of the tungsten atoms has three facial terminal oxygen atoms. Because of these two characteristics, which do not take into account possible protonation of the oxygen atoms, this intermediate is not stable and is transformed to $[\gamma\text{-SiW}_{10}\text{O}_{36}]^{8-}$ by rotation of the original ditungstic group and elimination of a water molecule.

It seems that the two dilacunary ions $[\beta\text{-SiW}_{10}\text{O}_{37}]^{10-}$ and $[\gamma\text{-SiW}_{10}\text{O}_{36}]^{8-}$ can be easily interconverted since the reverse transformation is initiated by coordination of Ni^{2+} ions.

The dimeric anion is considered to have a total charge of minus twelve based on charge balance considerations. This charge requires eight protons, which are assumed to be bound directly to surface oxygen atoms of **1**. Bond valence sum calculations allowed the assignment of specific binding sites

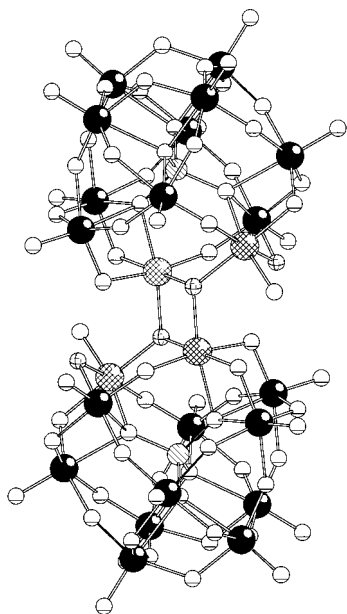


Figure 1. Ball and stick representation of $[\{\beta\text{-SiNi}_2\text{W}_{10}\text{O}_{36}(\text{OH})_2(\text{H}_2\text{O})_2\}]^{12-}$ (**1**). The two water molecules are represented by small empty spheres and the four OH groups are shown as small crosshatched spheres.

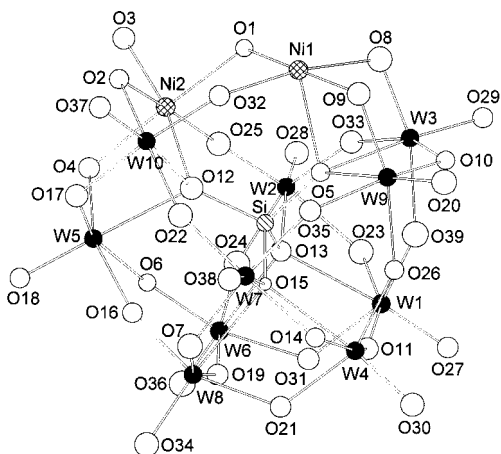


Figure 2. Ball and stick representation of a half-unit of $[\{\beta\text{-SiNi}_2\text{W}_{10}\text{O}_{36}(\text{OH})_2(\text{H}_2\text{O})_2\}]^{12-}$ (**1**) showing 50% probability ellipsoids and the labeling scheme.

for these protons.²¹ For O1, the summation of bond valences O1–Ni1 (0.33), O1–Ni2 (0.33) and O1–Ni1' (0.35) leads to a value of 1.01, strongly suggesting monoprotection. The O2 oxygen atom is doubly bridging Ni2 and W10, with distances equal to 2.03(2) and 2.02(2) Å, respectively. The respective bond valences are equal to 0.36 and 0.76, and the sum again suggests monoprotection. Ni2 is bound to O3, a terminal oxygen atom, with a distance equal to 2.03 (2) Å. The bond valence for O3 is equal to 0.37, which indicates that O3 is actually a molecule of water. All protonated oxygen atoms are therefore associated with Ni atoms. The occurrence of two OH groups and one molecule of water per half-unit of **1** is in agreement with the finding of six potassium cations in the lattice.

The twelve potassium counterions are bound to oxygens of **1** as well as to water molecules of crystallization, and their coordination numbers are 4 (K6), 5 (K3), 6 (K1, K2, K5) and 8 (K4), with $\text{K}\cdots\text{O}$ distances ranging from 2.65 to 2.99 Å.

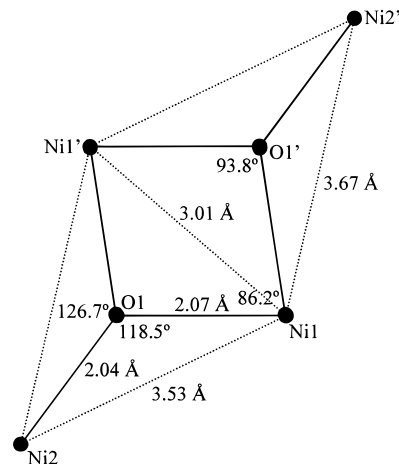


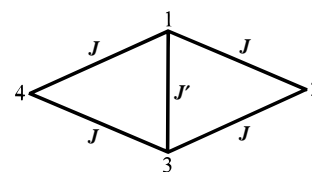
Figure 3. The central Ni_4O_2 unit of $[\{\beta\text{-SiNi}_2\text{W}_{10}\text{O}_{36}(\text{OH})_2(\text{H}_2\text{O})_2\}]^{12-}$ (**1**). All bond distances and angles as well as the Ni–Ni distances are shown. The Ni1–O1–Ni1'–O1' unit is planar, and the two bonds Ni2–O1 and Ni2'–O1' are projected on this plane (see text).

Polarography studies of **1** in acetate buffer indicated two well resolved reduction waves at -0.71 and -0.82 V (vs SCE), respectively. In the presence of **1**, reduction of the solvent takes place at -1.1 V, that is, at a potential about 200 mV more positive than the reduction potential of the pure buffer solution.

Magnetic Properties. Since **1** contains a well isolated central Ni_4 unit with an unprecedented geometry, it is of interest to investigate the magnetic properties of the title compound. Magnetization and magnetic susceptibility measurements are efficient methods for obtaining information about the magnetic interactions in spin clusters. The results of the magnetic measurements for $\text{K}_{12}[\{\beta\text{-SiNi}_2\text{W}_{10}\text{O}_{36}(\text{OH})_2(\text{H}_2\text{O})_2\}] \cdot 30\text{H}_2\text{O}$ are displayed in Figures 5 and 6, respectively. The magnetization at 2 K (Figure 5) shows a steep increase up to about 1 T and then starts to curve but without reaching saturation at 5 T. The temperature dependence of the magnetic susceptibility (Figure 6) shows an almost constant value of about 1.2×10^{-5} emu/g Oe between 290 and 50 K. Between 50 and 10 K, there is an exponential increase and below 10 K, there is a sharp increase, reaching a value of 4.8×10^{-5} emu/g Oe at 2 K.

Because the exchange interaction between the individual Ni^{2+} ions is mediated through the oxo-bridges linking them, it is important to identify all bond lengths and angles of the central Ni_4 unit (see Figure 3). There are three types of Ni–O–Ni angles, $93.8(7)^\circ$ (Ni1–O1–Ni1'), $118.5(8)^\circ$ (Ni1–O1–Ni2), $126.7(9)^\circ$ (Ni1'–O1–Ni2) and therefore also three types of Ni–Ni distances, 3.01 Å (Ni1–Ni1'), 3.53 Å (Ni1–Ni2) and 3.67 Å (Ni1'–Ni2). Because it is known that for Ni–O–Ni angles around 90° , ferromagnetic exchange is dominant and that for Ni–O–Ni angles around 120° , antiferromagnetic exchange is dominant, it can be expected that for **1** both types of exchange will contribute.^{11,22}

To analyze the observed magnetic properties of $\text{K}_{12}[\{\beta\text{-SiNi}_2\text{W}_{10}\text{O}_{36}(\text{OH})_2(\text{H}_2\text{O})_2\}] \cdot 30\text{H}_2\text{O}$, the following exchange scheme has been used:



exchange scheme

(21) Brown, I. D.; Altermatt, D. *Acta Crystallogr.* **1985**, *B41*, 244.

(22) Ginsberg, A. P. *Inorg. Chim. Acta Rev.* **1971**, *5*, 45.

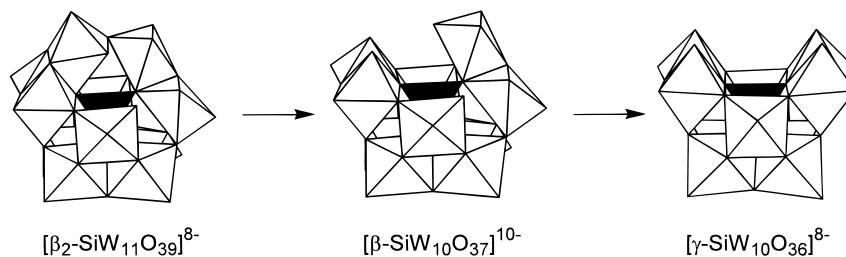


Figure 4. Polyhedral representation of the hydrolysis of $[\beta_2\text{-SiW}_{11}\text{O}_{39}]^{8-}$ to $[\gamma\text{-SiW}_{10}\text{O}_{36}]^{8-}$; the intermediate $[\beta\text{-SiW}_{10}\text{O}_{37}]^{10-}$ has not been isolated as a free species but appears in $[\{\beta\text{-SiNi}_2\text{W}_{10}\text{O}_{36}(\text{OH})_2(\text{H}_2\text{O})\}_2]^{12-}$ (**1**).

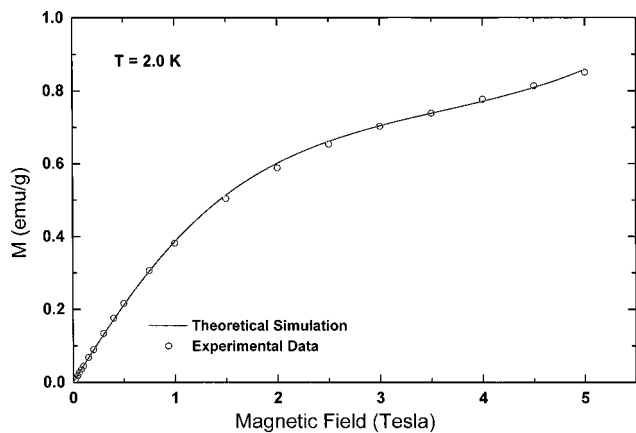


Figure 5. Plot of magnetization of $\text{K}_{12}[\{\beta\text{-SiNi}_2\text{W}_{10}\text{O}_{36}(\text{OH})_2(\text{H}_2\text{O})\}_2]\cdot 30\text{H}_2\text{O}$ at 2K.

The corners of the parallelogram with the numbers 1, 2, 3, and 4 symbolize the nickel ions Ni1, Ni2, Ni1' and Ni2'. The interaction between Ni1 and Ni1' is given by the coupling constant J' and because the interaction between Ni1 and Ni2 is expected to be similar to that of Ni1' and Ni2, both exchange interactions are described by the coupling constant J .

In the presence of an external magnetic field, the spin Hamiltonian for the tetrameric cluster is given by

$$H = g\mu_B(S_1 + S_2 + S_3 + S_4)H - 2J'S_1S_3 - 2J(S_1S_2 + S_1S_4 + S_2S_3 + S_3S_4) \quad (1)$$

where g is the Landé factor for Ni^{2+} and is equal to 2.3,²² μ_B is the Bohr magneton, and H is the external magnetic field. The energy levels of the spin Hamiltonian of eq 1 are given by

$$E(S_T, S_{12}, S_{34}, S_{13}, m, m') = -(m + m')g\mu_B H + J[S_{13}(S_{13} + 1) - 2S(S + 1)] + J[(S_T(S_T + 1) - S_{12}(S_{12} + 1) - S_{34}(S_{34} + 1))] \quad (2)$$

where $S_T = S_1 + S_2 + S_3 + S_4$ and $S_{kl} = S_k + S_l$ with $k, l = 1, 2, 3, 4$. For the Ni_4 core in **1** we have $S_1 = S_2 = S_3 = S_4 = 1$, $0 \leq S_{12} \leq 2$, $0 \leq S_{34} \leq 2$ and $|S_{12} - S_{34}| \leq S_T \leq S_{12} + S_{34}$. The value of the magnetization was then calculated by using its thermodynamic definition:

$$M = -k_B N_A T (\partial \ln(Z) / \partial H) \quad (3)$$

where Z is the partition function given by

$$Z = \sum_{i,j} e^{(-E_{ij}/k_B T)} \quad (4)$$

Figure 5 shows the magnetization measurements of $\text{K}_{12}[\{\beta\text{-SiNi}_2\text{W}_{10}\text{O}_{36}(\text{OH})_2(\text{H}_2\text{O})\}_2]\cdot 30\text{H}_2\text{O}$ at 2K. The experimental data were fitted using eq 3, and the values of the exchange

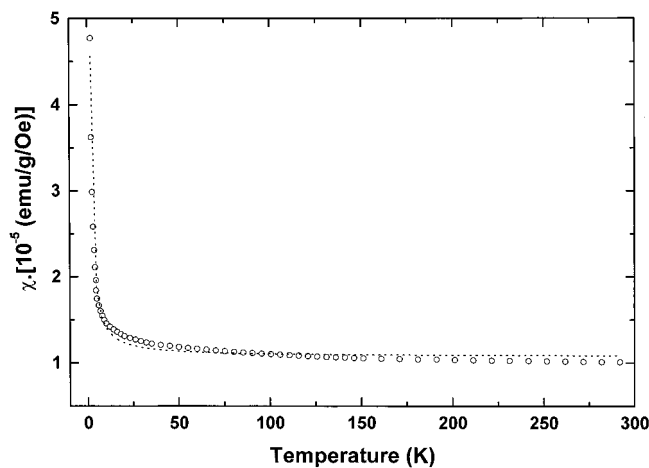


Figure 6. Plot of the effective magnetic moment as a function of temperature for $\text{K}_{12}[\{\beta\text{-SiNi}_2\text{W}_{10}\text{O}_{36}(\text{OH})_2(\text{H}_2\text{O})\}_2]\cdot 30\text{H}_2\text{O}$ in a constant magnetic field of 1 kG.

interactions were determined to be $J' = 4.46 \text{ cm}^{-1}$ and $J = -0.64 \text{ cm}^{-1}$. For values of $J'/J < -2$, the ground spin state is a mixture of spin states with $S = 2, 1$ and 0 . The magnetic susceptibility per mole is given by Gladfelter et al.:²⁴

$$\chi_{\text{cluster}} = \frac{\sum_i (2S + 1)S(S + 1)e^{(-E_i/k_B T)}}{(4N_A g^2 \mu_B^2 / 3k_B T)S(S + 1) \sum_i (2S + 1)e^{(-E_i/k_B T)}} \quad (5)$$

Figure 6 shows the magnetic susceptibility in the temperature range from 2 to 290 K. The dotted line represents the best fit to the experimental data. The exchange constants obtained are $J' = 4.14 \text{ cm}^{-1}$ and $J = -0.65 \text{ cm}^{-1}$, respectively. To account for intercluster interactions, we included the mean field correction which was found to be weakly antiferromagnetic ($\theta = -0.65 \text{ cm}^{-1}$).

Out of the few known Ni-containing polyoxotungstates there are two structural types which also contain four Ni^{2+} ions per polyanion. These are the Finke-type polyoxoanions $[\text{Ni}_4(\text{H}_2\text{O})_2(\text{PW}_9\text{O}_{34})_2]^{10-}$ and $[\text{Ni}_4(\text{H}_2\text{O})_2(\text{P}_2\text{W}_{15}\text{O}_{56})_2]^{16-}$ and the recently reported polyanion $[\text{H}_2\text{PW}_9\text{Ni}_4\text{O}_{34}(\text{OH})_3(\text{H}_2\text{O})_6]^{2-}$ which contains a Ni_4O_4 cubane unit.¹³ It is of interest to compare the magnetic properties of these species with those of **1**. The geometry of the magnetic tetrameric core in the Finke ions is a rhomb, and because all Ni—O—Ni angles are around $90^\circ - 100^\circ$ ferromagnetic exchange interactions are observed, leading to

(23) Abragam, A.; Bleaney, B. *Electron Paramagnetic Resonance of Transition Ions*, Oxford University Press: London, 1970.

(24) Gladfelter, W. L.; Lynch, M. W.; Schaefer, W. P.; Hendrickson, D. N.; Gray, H. B. *Inorg. Chem.* **1981**, *20*, 2390.

an $S = 4$ spin ground state. Also, in the cubane-containing cluster of Kortz et al., the Ni–O–Ni angles are in the range which leads to ferromagnetic interaction between the Ni centers. Therefore, the magnetic properties of **1** are clearly different from those of the other polyoxometalates containing four Ni²⁺ ions. The reason is the unique arrangement of the Ni-centers in **1**, leading to both ferromagnetic and antiferromagnetic intramolecular interactions.

Conclusions

A novel Ni-containing silicotungstate has been synthesized, and single-crystal X-ray crystallography revealed that the new structure consists of two [β -SiNi₂W₁₀O₃₆(OH)₂(H₂O)] Keggin moieties linked via two OH bridging groups. The formation of the new anion **1** is derived from the [γ -SiW₁₀O₃₆]⁸⁻ lacunary anion, and the synthesis of **1** involves therefore insertion of Ni²⁺, isomerization, and dimerization. The title compound contains

the largest number of paramagnetic transition metals of all silicotungstates known. In addition, the central Ni₄O₂ unit has an unprecedented geometry, and its magnetic properties are a combination of both ferromagnetic and antiferromagnetic exchange interactions in accordance with the observed Ni–O–Ni bond angles.

Acknowledgment. U.K. thanks the French Ministry of Education for an Alfred Kastler fellowship. We thank Mr. M. Nogues for doing the magnetic measurements. Figures 1, 2 and 4 were generated by Diamond Version 2.1a (copyright Crystal Impact GbR).

Supporting Information Available: One X-ray crystallographic file, in CIF format. This material is available free of charge via the Internet at <http://pubs.acs.org>.

IC990008D